

## Significant Inversions and Rapid In Situ Cooling at a Well-Sited Oklahoma Mesonet Station

ERIC D. HUNT, JEFFREY B. BASARA, AND CYNTHIA R. MORGAN

*Oklahoma Climatological Survey, University of Oklahoma, Norman, Oklahoma*

(Manuscript received 5 December 2005, in final form 14 July 2006)

### ABSTRACT

The El Reno Oklahoma Mesonet (ELRE) site is one of a few Oklahoma Mesonet sites that has measured inversions of 10°C or greater between 1.5 and 9 m. Historical analyses revealed that strong inversions at ELRE have occurred because of rapid cooling near the surface shortly after sunset when conditions are calm, clear, and dry. In addition, ELRE is a very well sited station and is located on very slightly sloped terrain with no obstructions nearby. Four Portable Automated Research Micrometeorological Stations (PARMS) were deployed along a transect orthogonal to ELRE for 3 months in the spring of 2005 to quantify the micrometeorological processes that caused rapid cooling and subsequent strong inversions to form. One-minute data collected from the PARMS and ELRE during the study verified the variability and duration of strong inversion events. Analyses from the field study also revealed that significant horizontal and vertical differences in air temperature and wind speed existed during periods of differential wind speeds between the PARMS and ELRE.

### 1. Introduction

At night longwave emission cools the land surface more quickly than the air above it and the boundary layer can become stable with cold air trapped near the surface (Hartmann 1994). Low-level nocturnal inversions are a common occurrence during these stable atmospheric conditions. Some inversions are induced by synoptic-scale processes (Groen 1947; Fiebrich and Crawford 1998), while others are influenced by local conditions, such as terrain and landscape (Gustavsson et al. 1998; Fiebrich and Crawford 1998), and typically impact a very small area in the lowest levels of the troposphere. Geiger et al. (1995) showed that a surface inversion increases in strength until sunrise and often reaches heights of 100 m or greater. Within the overall inversion, an inversion sublayer also forms; the inversion sublayer has an annual average height of 21 m above the surface. Further, the authors demonstrated that while the vertical extent of the inversion increases through the night, the inversion sublayer develops rap-

idly during the first 1–2 h following sunset and then becomes relatively stable. Likewise, the maximum temperature gradient of the inversion sublayer occurs within the first 1–2 h after sunset and then decreases somewhat for the remainder of the night.

Inversions that occur within the inversion sublayer are a result of radiational cooling (Geiger et al. 1995). The air aloft within the overall inversion cools as a result of conduction and weak convective or shear-induced mixing until sunrise the following day, while strong temperature gradients in the inversion sublayer occur when the wind profile is very weak. Hartmann (1994) demonstrated that high vertical stability is present with nocturnal inversions and the turbulent exchange of energy with the surface is suppressed. Latent and sensible heat fluxes are also suppressed allowing radiative forcing to dominate. Thus, the air just above the surface continues to cool rapidly forming a large vertical temperature gradient between the air near the surface and the air aloft; the process is further accentuated during clear sky and dry conditions as longwave loss to the atmosphere is large (Perrotin 1920; Groen 1947; Hartmann 1994; Geiger et al. 1995). Geiger et al. (1995) further showed that wind speeds and inversion strength are interrelated as increases in wind speed are followed by a breakdown of the inversion.

At the surface, studies have documented different

---

*Corresponding author address:* Dr. Jeffrey B. Basara, Oklahoma Climatological Survey, 120 David L. Boren Blvd., Suite 2900, Norman, OK 73072-7305.  
E-mail: jbasara@ou.edu

types of cooling in different regions. Gustavsson et al. (1998) found that very large temperature variations can occur during clear nights with horizontal variations as large as 15°C across a 22-km route of their study area in southwest Sweden. It is widely accepted that the best conditions for nocturnal cooling are clear nights with calm or light winds, little moisture, and stable atmospheric conditions (Thompson 1986; Gudiksen et al. 1992; Fiebrich and Crawford 1998). The primary documented mechanisms for nocturnal cooling include cold-air drainage (Thompson 1986; Gudiksen et al. 1992; Kondo 1995), katabatic flow (Thompson 1986; Feng and Chen 2001), and in situ cooling (Thompson 1986; Gustavsson et al. 1998; Fiebrich and Crawford 1998, 2001; Clements et al. 2003).

Cold-air drainage occurs when cold air flows downhill from gravity. Thompson (1986) found that a gradient of 1 m of elevation rise over a horizontal distance of 200 m was not enough to produce cold-air drainage and that large gradients are needed for this type of flow to occur. A study by Kondo (1995) on the Kanto Plain of Japan's Honshu Island showed that cold-air drainage began approximately 2 h after sunset as the cold dense air flowed off the nearby mountain and across the Kanto Plain at nearly 4.7 m s<sup>-1</sup>. Gudiksen et al. (1992) studied the nocturnal drainage flows within the Mesa Creek Valley in western Colorado and found that increased atmospheric moisture and wind speeds greater than 5 m s<sup>-1</sup> hindered the drainage flows.

Within mountainous regions, higher elevations often cool faster than the lower elevations and katabatic winds develop that advect cooler air into the valleys. The pressure over the warmer valley surface is lower than the pressure over the cooler air that is on the top or side of the hill. This creates a pressure gradient and a downslope wind begins. For the katabatic flow to maintain itself, the valley air must always be warmer than the air being advected into the valley so that the pressure gradient is maintained (Thompson 1986). The katabatic wind can be measured within a few meters of the surface and is normally very weak. Thompson (1986) was able to measure a very weak katabatic wind during the winter when the air over a lake located at the bottom of a hill was warmer than the air on the side of the hill. Feng and Chen (2001) used a numerical model to study the katabatic flows on the island of Hawaii and revealed that after 2 h of nocturnal cooling the katabatic flow reached the coast; as the night progressed, the flow spread several miles offshore.

In situ cooling occurs when the air near the surface does not mix with the surrounding air and is typically associated with wind obstructions, such as hills and

trees. These obstructions block the wind and can aid in the creation of large horizontal temperature gradients if skies are clear and winds are light. In situ cooling begins and is most intense right after sunset. Measurements by Thompson (1986) showed that the sheltering effect of topography could be responsible for large temperature variations while Gustavsson et al. (1998) found that very large temperature variations are possible within 1 h of cooling. In situ cooling has also been found to be a major reason for cold-air pools. Gustavsson et al. (1998) demonstrated that in valleys, the greatest cooling occurred during the first 2 h after sunset and during the remainder of the night the rate slowed. Andre and Mahrt (1982) divided the nocturnal boundary layer into the lower (turbulent) layer and the upper layer. The study found that weak slopes can affect nocturnal cooling rates and that the lower layer varied slowly throughout the night and was different from night to night.

In situ cooling has been found to cause large vertical temperature gradients near sunset at Oklahoma Mesonet sites (Fiebrich and Crawford 2001). Several sites across Oklahoma have been documented as being susceptible to intense radiational cooling and, although rare, the Oklahoma Mesonet has measured inversions over 10°C between 1.5 and 9 m at some locations. Fiebrich and Crawford (1998) found that inversions with magnitudes greater than 3°C were frequent, inversions of at least 6°C were not as common, and inversions of at least 10°C occurred only 6 times from 29 February 1995 to 1 March 1996. Fiebrich and Crawford (1998) also found that winter was the most prominent season for strong inversions.

One mesonet site in particular, the El Reno site (ELRE), has yielded strong nocturnal inversions as well as intense rapid cooling on a regular basis. However, the site has puzzled Oklahoma Mesonet personnel for years because it lacks the typical local features associated with such cooling episodes (e.g., obstructions, terrain). In fact, ELRE is installed at a location that greatly exceeds the standard siting requirements established by the World Meteorological Organization (WMO 1983). Siting requirements listed by WMO (1983) include, but are not limited to, flat, open ground with natural cover and a horizontal distance of at least 4 times the height of the nearest vertical obstruction. Thus, the focus of this paper is to document the development of inversions and rapid cooling at ELRE and to diagnose the physical processes that contribute to the unique conditions observed. Extensive analysis of historical climate data is utilized as well as observations from an intense field study near and around the ELRE site during January–April 2005.

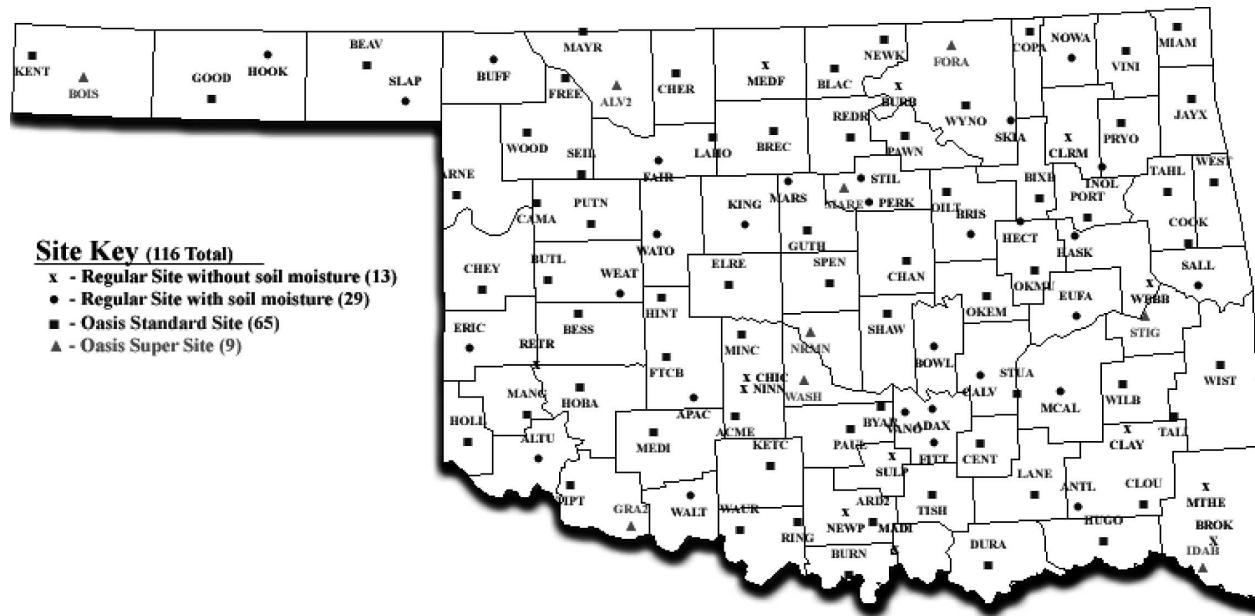


FIG. 1. The Oklahoma Mesonet.

## 2. Data and methods

### a. The Oklahoma Mesonet

The Oklahoma Mesonet consists of 116 remote meteorological stations (Fig. 1) across Oklahoma (Brock et al. 1995; McPherson et al. 2007). Each site records air temperature and relative humidity at 1.5 m, wind speed and wind direction at 10 m, rainfall, downwelling solar radiation, soil temperature, soil moisture (except at sites with poor soil conditions), and barometric pressure. Of the 116 stations, 100 also measure air temperature at 9 m and wind speed at 9 and 2 m (McPherson et al. 2007). Mesonet sites are powered by a solar panel and a battery. Data are relayed to a base via radio then transmitted through the Oklahoma Law Enforcement Telecommunications System (OLETS) to a central processing facility in Norman, Oklahoma. The data are then processed through rigorous automated and manual quality assurance (QA) processes (Shafer et al. 2000) and archived, and products are generated for distribution via the Internet (McPherson et al. 2007; [www.mesonet.org](http://www.mesonet.org)). During typical operation, each mesonet site records averaged data observations at 5–30-min intervals, depending on the variable measured, and reports every 5 min. Oklahoma Mesonet stations are installed across a variety of vegetation, soil, terrain, and climate conditions. Even so, rigorous siting requirements exist for mesonet stations such that each site must be representative of the surrounding conditions, a distance of approximately 300 m from the nearest obstruction, and in an area with no more than 5% change

in elevation (Brock et al. 1995; Shafer et al. 2000; McPherson et al. 2007).

### b. The ELRE site

The ELRE site is located approximately 8 km west-northwest of El Reno, Oklahoma. The land surrounding the site is open terrain covered by natural tallgrass prairie and is very slightly sloped from east to west. During the study, high-resolution elevation data were collected near and around the ELRE site at approximately 1200 locations. The observations (Fig. 2) clearly reveal the minor elevation gradient oriented east (lower elevations) to west (higher elevations).

A climatological study of ELRE was completed using 5-min-averaged data collected from January 2000 through December 2004 with particular focus on observations of air temperature at 1.5 and 9 m, wind speed at 2 and 10 m, wind speed and wind direction at 10 m, and relative humidity at 1.5 m. From October 2004 through April 2005, 1-min-averaged data were recorded at ELRE and studied during nights with inversions greater than 5°C. Additional site information and photos for ELRE were available online at the time of writing (<http://www.mesonet.org/sites/sitedescription.php?site=ELRE&dir=pr>).

### c. Portable Automated Research Micrometeorological Stations (PARMS)

Four PARMS (Basara 2005) were deployed along an east–west transect near ELRE. The PARMS measured

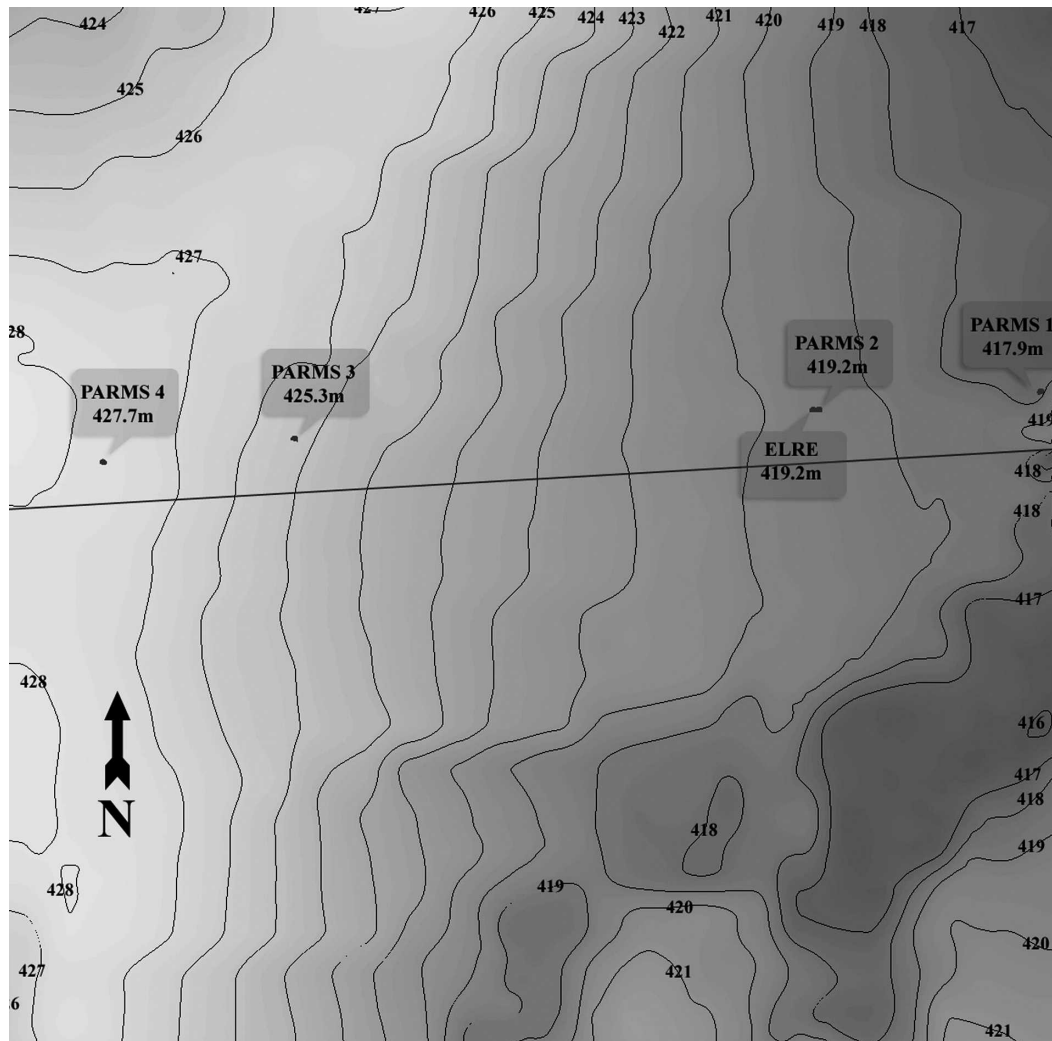


FIG. 2. Topographic map and deployment of the PARMS near the ELRE site. Horizontal distance between PARMS 1 and PARMS 4 is approximately 700 m.

numerous meteorological variables at 1-min-averaged intervals, including air temperature and relative humidity at 1.5 m, the  $u$ ,  $v$ , and  $w$  wind components at 2 m, solar radiation, net radiation, and surface skin temperature. Table 1 documents the variables measured at the

TABLE 1. Instruments installed on PARMS.

Variable	Instrument
1.5-m air temperature and humidity	Themometrics FastAir and Vaisala HMP45A
Surface skin temperature	Apogee IRTS-P
2-m 3D wind speed and direction	RM Young 81000 sonic anemometer
Solar radiation	Li-Cor 200S Pyranometer
Net radiation	Kipp and Zonen NR-Lite net radiometer

PARMS and the instruments used. The PARMS were deployed during an intensive field study from January through March 2005 along an east–west-oriented transect (Fig. 2) and spaced at intervals shown in Table 2. Unfortunately, the sonic anemometer at PARMS 1 failed a few weeks into the field study and wind data were unusable after 21 February 2005.

TABLE 2. The distance between ELRE and the PARMS in meters.

	ELRE	PARMS 1	PARMS 2	PARMS 3	PARMS 4
ELRE	—	171	10	387	529
PARMS 1	171	—	167	557	699
PARMS 2	10	167	—	391	533
PARMS 3	387	557	391	—	143
PARMS 4	529	699	533	143	—

TABLE 3. RMS differences between PARMs for the  $u$  wind component ( $u$ ), the  $v$  wind component ( $v$ ), the  $w$  wind component ( $w$ ), air temperature measured by the Thermometrics Fasttherm (TAIR 1), air temperature measured by the Vaisala HMP45A (TAIR 2), RH, net radiation (RNET), and surface skin temperature (IRT).

	$u$ ( $\text{m s}^{-1}$ )	$v$ ( $\text{m s}^{-1}$ )	$w$ ( $\text{m s}^{-1}$ )	TAIR 1 ( $^{\circ}\text{C}$ )	TAIR 2 ( $^{\circ}\text{C}$ )	RH (%)	RNET ( $\text{W m}^{-2}$ )	IRT ( $^{\circ}\text{C}$ )
PARMS 1 vs PARMs 2	0.26	0.19	0.08	0.11	0.08	1.03	3.79	0.83
PARMS 1 vs PARMs 3	0.24	0.27	0.07	0.36	0.11	1.95	7.87	0.83
PARMS 1 vs PARMs 4	0.28	0.33	0.08	0.22	0.13	1.34	9.92	1.26
PARMS 2 vs PARMs 3	0.20	0.23	0.08	0.29	0.07	1.08	7.26	0.58
PARMS 2 vs PARMs 4	0.26	0.30	0.08	0.17	0.09	0.54	9.38	0.75
PARMS 3 vs PARMs 4	0.11	0.18	0.07	0.21	0.05	0.94	4.10	0.63

The utility of the PARMs for the intensive field study was twofold; the PARMs include two separate instruments that measure air temperature at 1.5 m (Table 1; Basara 2005). Thus, redundant measurements were available for validating the observed conditions. Unlike the cup anemometer installed at 2 m at ELRE, which has a minimum wind speed threshold of  $0.5 \text{ m s}^{-1}$ , the 3D sonic anemometer on each PARMs has a minimum threshold of  $0.01 \text{ m s}^{-1}$ , an accuracy of  $\pm 0.05 \text{ m s}^{-1}$  from 0 to  $30 \text{ m s}^{-1}$ , and a resolution of  $0.1 \text{ m s}^{-1}$ . Thus, the PARMs recorded higher-resolution near-surface wind observations needed for this study.

Prior to deployment at ELRE, the PARMs underwent a field calibration whereby the sites were arranged side by side and data were collected for nearly 2 weeks. The purpose of the field calibration was to quantify the variability of the measurements collected by the PARMs in a controlled environment. Overall, very minor differences were noted between PARMs for the variables utilized in this study (Table 3). Therefore, the differences observed during the field study were a result of physical processes and not instrumentation bias.

### 3. Historical inversion climatology

#### a. Historical overview

Inversions at ELRE have often exceeded  $5.0^{\circ}\text{C}$  between the 1.5- and 9-m levels (defined as a *significant inversion* for this study). Five years of data from January 2000 to December 2004 were analyzed to determine the strength and number of inversions at ELRE relative to surrounding Oklahoma Mesonet sites (Table 4). Significant inversions at ELRE were observed on 273 nights during the 5-yr study period, as compared with a median of 55 nights for the surrounding mesonet sites. Inversions have been recorded throughout the entire year at ELRE but are most prevalent in the meteorological autumn, with a peak in September (Fig. 3). Autumn seemed to be the optimal time for significant inversions as strong ridges of high pressure would often

settle into the southern plains following the passage of a cold front. The clear, calm, dry, yet relatively warm conditions left in the wake of early autumn cold frontal passages were ideal conditions for the formation of significant inversions.

The nature of the inversions at ELRE is tied to the rate of cooling at 1.5 m versus other mesonet sites. Table 5 shows the mean temperature difference at 1.5 and 9 m between ELRE and the surrounding sites of Spencer (SPEN), Minco (MINC), Kingfisher (KING), and Hinton (HINT) at the time of the peak of the inversions at ELRE between January 2000 and December 2004. At 9 m the differences were minimal and, on average, ELRE was slightly warmer than KING at the peak of the inversion events. However, at 1.5 m ELRE was substantially cooler than the surrounding sites with differences ranging, on average, from  $3.84^{\circ}$  to  $6.26^{\circ}\text{C}$ . Thus, during inversion events, the 9-m temperature was very similar among the sites while the rate of cooling at 1.5 m was dramatically different.

ELRE has recorded some of the strongest inversions observed at Oklahoma Mesonet sites. The inversions at ELRE were unique regarding the time of night when they occurred. Unlike typical nocturnal inversions that usually reach maximum strength shortly before sunrise (Geiger et al. 1995), the significant inversions at ELRE usually occurred in the first few hours following sunset.

Inspection of past surface conditions at ELRE as well

TABLE 4. Number of days with significant inversions by meteorological season and maximum inversion recorded at ELRE and surrounding sites from 0000 UTC 1 Jan 2000 to 1200 UTC 12 Dec 2004 (here ID is identifier).

Total No. of inversions at ELRE and surrounding mesonet sites					
Site ID	Spring	Summer	Autumn	Winter	Total
ELRE	54	28	101	89	273
HINT	16	1	17	14	48
KING	21	1	9	30	61
SPEN	21	5	37	21	84
MINC	0	1	4	2	7

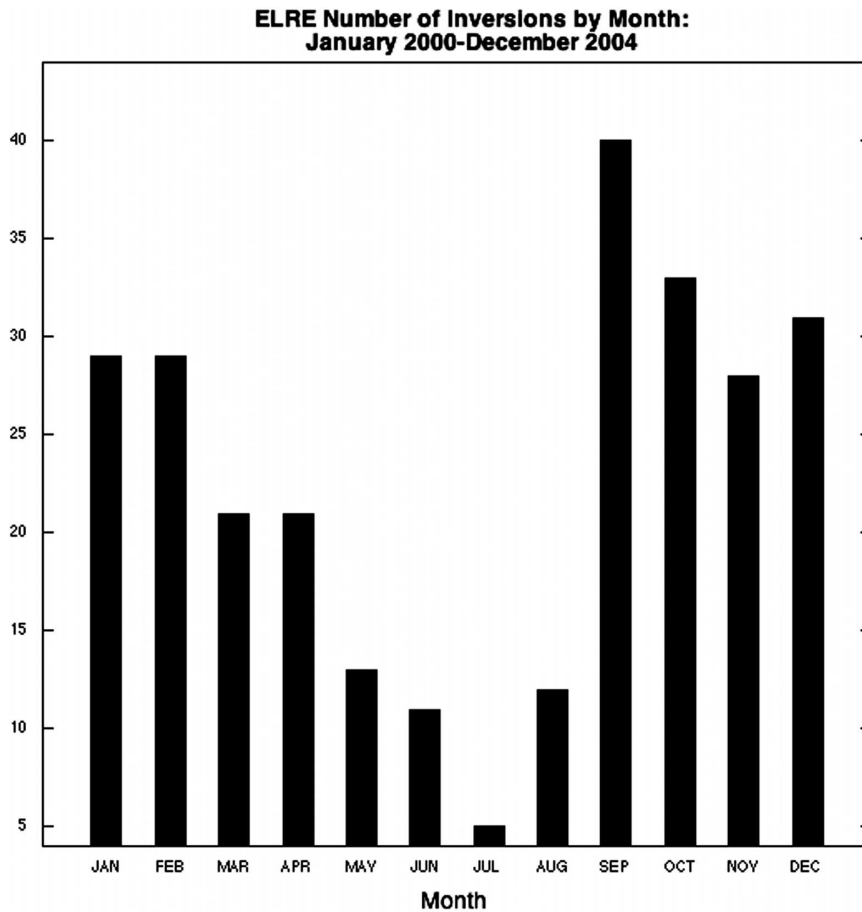


FIG. 3. Number of significant inversions by month at ELRE from January 2000 to December 2004.

as SPEN, MINC, KING, and HINT did not reveal any significant or consistent differences that would create such atmospheric anomalies. All Oklahoma Mesonet sites are installed over native vegetation and the surface conditions inside the site are maintained to match those outside as closely as possible (Fiebrich et al. 2006; McPherson et al. 2007). Throughout the year, vegetation height at ELRE and the surrounding sites changed because of the natural variation of land cover. While subtle differences occurred from site to site, a consis-

TABLE 5. Mean difference in TAIR ( $^{\circ}\text{C}$ ) at 1.5 and 9 m between surrounding sites and ELRE at the time of peak inversion strength.

Site ID	Difference in 1.5 m TAIR ( $^{\circ}\text{C}$ )	Difference in 9 m TAIR ( $^{\circ}\text{C}$ )
SPEN	4.25	0.46
KING	3.84	-0.49
HINT	4.55	0.32
MINC	6.26	1.24

tent pattern that highlighted ELRE versus the other sites was not found. In addition, for these sites little if any bare soil was exposed regardless of season. Additional metadata concerning each site, including historical site photos and soil characterizations, were located online at the time of writing (<http://www.mesonet.org/sites/>).

#### b. Historical example

Consider the example that occurred on 9 September 2004, which is the strongest inversion observed to date at ELRE. Conditions at 0000 UTC (approximately 45 min prior to sunset) 9 September 2004 included clear skies, a large dewpoint depression ( $\sim 18^{\circ}\text{C}$ ), and light northeast winds. Following sunset, the wind speed at 2 m became calm and the air temperature at 1.5 m began to cool rapidly (Fig. 4). Conversely, the air temperature at 9 m cooled at a much slower rate and a significant inversion formed by 0100 UTC (15 min after sunset). Calm conditions prevailed during the next hour and the

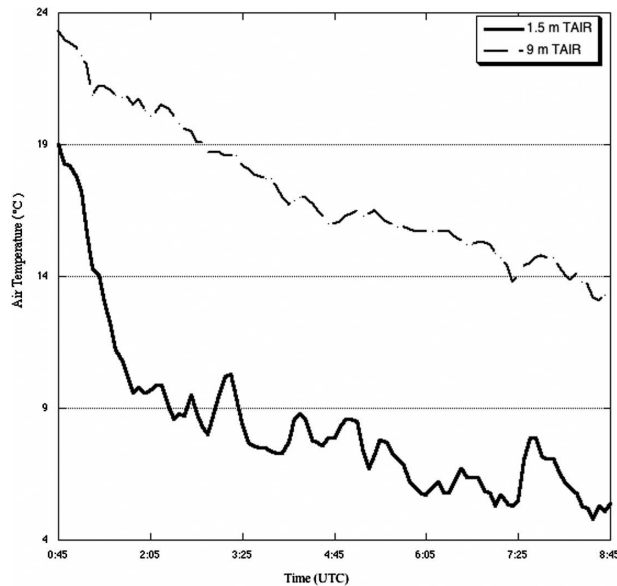


FIG. 4. Air temperature at 1.5 and 9 m at ELRE from 0045 to 0845 UTC 9 Sep 2004.

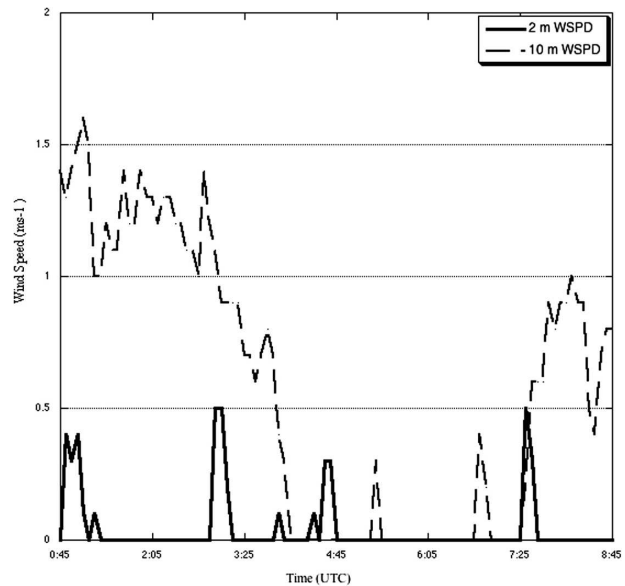


FIG. 5. Wind speed at 2 and 10 m at ELRE from 0045 to 0845 UTC 9 Sep 2004.

air temperature at 1.5 m continued to decrease while inversion strength intensified. The inversion reached a maximum magnitude at 0230 UTC with a difference between the 1.5- and 9-m air temperature values of 11°C. During the inversion, wind speed values at 2 m were calm (or very near calm) during the first hour after sunset while at 10 m were slightly stronger, allowing minor turbulent mixing to occur (Fig. 5).

During the 9 September 2004 case, ELRE was substantially cooler than surrounding Oklahoma Mesonet sites during the time of the inversion. For example, the 1.5-m air temperature at ELRE was 8.8°C at the time of the maximum inversion, while the next coolest surrounding mesonet site was SPEN at 15.9°C. ELRE was not only much cooler than surrounding mesonet sites, it was also the coldest mesonet site in the state (Fig. 6) and remained so for a few hours before sites in the far northern and western sections of Oklahoma became cooler. Additionally, similar trends have been noted on numerous other evenings when rapid cooling occurred at ELRE. Figure 7 shows the air temperature at ELRE in comparison with surrounding mesonet sites in central Oklahoma on 9 September 2004. After the inversion reached a maximum magnitude, the cooling rate sharply decreased and the air temperature fluctuated for the remainder of the night; the fluctuations in air temperature were highly correlated with fluctuations in the wind speed. Thus, periods of calm winds at 2 m allowed air temperature values to decrease while periods of increased wind speeds allowed for turbulent mixing and increased air temperature values. Eventually, as

the night progressed, the air temperature at ELRE became more comparable to air temperature values at surrounding mesonet sites (Fig. 7). Once the rapid surface cooling ceased at ELRE because of slightly stronger wind speeds, the inversion strength slowly decreased. Thus, even though the inversion remained very strong for several hours on 9 September 2004, the magnitude of the significant inversion decreased when the wind speed values increased (Figs. 4 and 5). Historical analysis is consistent with this sequence of events, confirming that during strong inversion events, the difference in air temperature at 1.5 m between ELRE and surrounding mesonet sites typically decreases to a minimum just prior to sunrise.

#### 4. Field study analysis

Four PARMs were placed along a transect orthogonal to the slope near ELRE for a 3-month period from 23 January 2005 to 19 April 2005. PARMs 1 was located at the east end of the transect at the lowest elevation while PARMs 2 was collocated with the ELRE site. PARMs 3 was installed in an area representing the greatest slope to the local terrain and PARMs 4 was deployed at the west end of the transect near the apex of the local terrain. The overall length of the transect spanned 699 m with an elevation change of approximately 10 m (Fig. 2; Table 2). During the field study, ELRE recorded significant inversions on 10 occasions (Table 6). The PARMs also observed a horizontal tem-

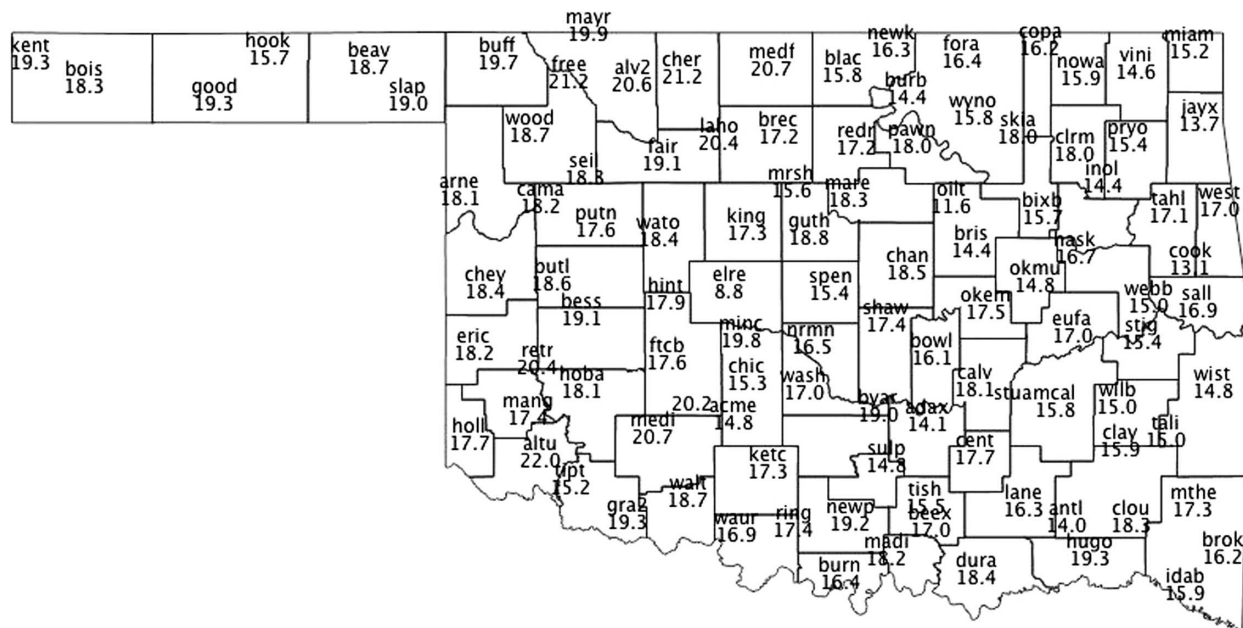


FIG. 6. Air temperature at 1.5 m at 0230 UTC 9 Sep 2004.

perature difference across the slope of  $5^{\circ}\text{C}$  or greater during five of the inversion events (Fig. 8). One-minute data from the PARMS and ELRE and the placement of the four PARMS allowed for further analysis of air temperature, wind speed, etc. along the slight grade of slope during nights with strong inversions. Clear to mostly clear skies were observed shortly before and during the time of significant inversions during all cases over the 3-month field study.

#### a. Dewpoint depression

Large dewpoint depressions often aid strong radiational cooling (Ahrens 2000) and were an important factor in nearly all of the inversion cases observed by the PARMS. Table 6 shows the dewpoint depression observed by ELRE at 0000 UTC preceding each inversion case as well as the elapsed time from sunset to the development of the significant inversion. Significant inversions also tended to occur more quickly with larger dewpoint depressions. For example, the  $20.2^{\circ}\text{C}$  dewpoint depression observed at 0000 UTC 13 March 2005 corresponded to the shortest amount of elapsed time from sunset to a significant inversion.

#### b. Wind speed

Reduced wind speeds at ELRE yielded less mixing. Historical analysis revealed that when wind speeds became calm at ELRE, strong inversions often formed. While wind speeds were light at all of the PARMS on

nights with significant inversions during the field study, some variability existed on different occasions. Figure 9a demonstrates the wind speed at ELRE for all 10 cases at the time of the maximum inversion between 1.5 and 9 m, while Fig. 9b shows the wind speed at the time of the maximum horizontal temperature difference between the PARMS. For every case observed during the field study, the wind speed at PARMS 2 and the 2-m wind speed at ELRE were  $1.5\text{ m s}^{-1}$  or less during the time of the maximum inversion. In addition, the maximum difference in temperature between the PARMS was always between one of the sites located at the bottom of the slope (1 or 2) and one of the sites situated near or at the top of the slope (3 or 4).

Overall wind speed values observed at PARMS 2 and ELRE during the formation of significant inversions were very weak and markedly different than the 10-m wind speed values observed at ELRE. This difference in wind speed appeared to be a primary cause for the formation of significant inversions. The very light wind speeds at 2 m yielded little mixing at the time of the maximum inversion. As a result of the lack of mixing, strong radiational cooling occurred. Hence, air temperatures at 1.5 m cooled rapidly while temperatures cooled more slowly at 9 m, where slightly greater wind speeds and mixing inhibit rapid cooling. Thus, the rapid cooling preceded the formation of the nocturnal inversion.

Wind speed differences leading to differential cooling also contributed to strong horizontal temperature



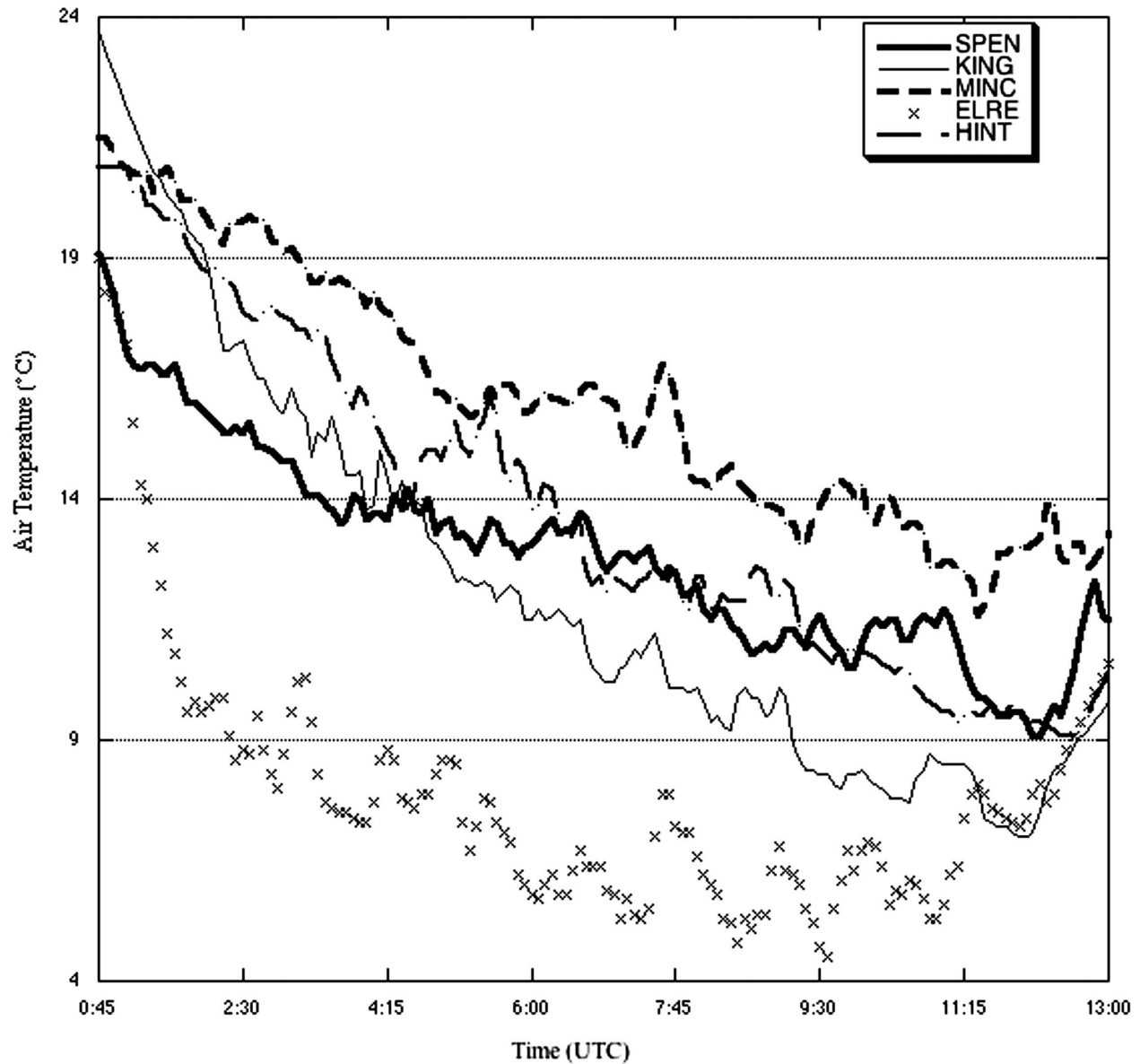


FIG. 7. Air temperature at 1.5 m from 0045 to 1300 UTC 9 Sep 2004 at ELRE and surrounding Oklahoma Mesonet sites.

differences that often formed between the PARMs. However, even though the horizontal temperature differences and maximum inversions were driven by similar processes, they did not occur simultaneously. Additionally, the magnitude of the horizontal temperature difference was usually a few degrees less than that of the maximum inversion strength (Fig. 8). The large horizontal temperature differences (i.e.,  $>5^{\circ}\text{C}$ ) only occurred when wind speeds were very light at the bottom of the slope when compared with the PARMs near the top of the slope. As such, the difference in wind speed between the PARMs also resulted in a difference in mixing between the sites. Higher wind speeds at

PARMs 3 and 4 led to increased mixing causing the air temperature to decrease slowly, remain static, or even rise slightly, despite radiational cooling. Conversely, wind speeds at PARMs 1 and 2 were minimal, mixing was minimized, and air temperatures cooled more rapidly. Even so, the large differences between PARMs normally did not last longer than 10 min, as even slight fluctuations in wind speed caused air temperature differences between PARMs to become negligible. Figures 10a,b demonstrate the impact of wind speed differences on the horizontal temperature difference between PARMs 2 and 4 on 28 March 2005. The largest difference in air temperature among the PARMs

TABLE 6. Dewpoint depression at 0000 UTC and elapsed time from sunset to the start of a significant inversion for all 10 cases.

Inversion No.	Date of inversion	Dewpoint depression	Elapsed time from sunset to significant inversion
Inversion 1	26 Jan 2005	8.2°C	82 min
Inversion 2	3 Feb 2005	5.0°C	346 min
Inversion 3	4 Feb 2005	6.2°C	52 min
Inversion 4	14 Feb 2005	14.7°C	42 min
Inversion 5	21 Feb 2005	13.2°C	413 min
Inversion 6	13 Mar 2005	20.2°C	21 min
Inversion 7	28 Mar 2005	11.9°C	136 min
Inversion 8	2 Apr 2005	18.7°C	59 min
Inversion 9	8 Apr 2005	15.5°C	57 min
Inversion 10	13 Apr 2005	19.0°C	72 min

shown in Fig. 9a corresponds to the largest difference in wind speed shown in Fig. 9b. Figures 10a,b also demonstrate the strong correlation between wind speed and air temperature (i.e., decreases in wind speed yielded a decrease in air temperature at the PARMS).

### c. Wind direction

Wind direction also contributed to the formation of significant inversions and horizontal temperature differences. While no specific wind direction was necessary for the formation of a significant inversion, a general westerly and southerly component to the wind was very common at all PARMS on nights with significant inversions. At times, inversion strength would increase when wind direction became southwesterly at the PARMS. For example, on 28 March 2005, even though the wind speed at PARMS 2 was generally less than  $1 \text{ m s}^{-1}$ , the inversion was approximately  $3^\circ$  to  $4^\circ\text{C}$ . However, as wind direction veered to the southwest

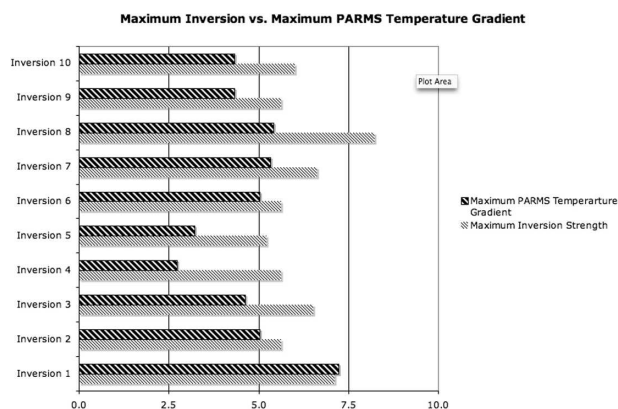


FIG. 8. The maximum strength of inversions at ELRE between 1.5 and 9 m in comparison with the maximum temperature difference observed between the PARMS.

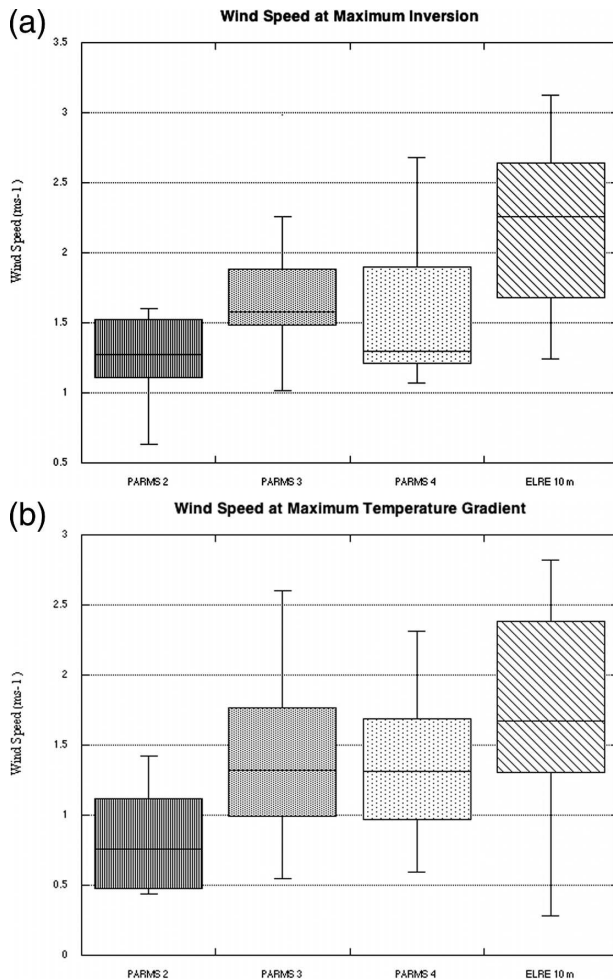


FIG. 9. (a) Wind speed observed at 2 m at the PARMS and the 10 m wind speed of ELRE observed at the time of the maximum inversion during the field study. (b) Wind speed observed at 2 m at the PARMS and the 10-m wind speed of ELRE observed at the time of the maximum temperature difference during the field study.

(Fig. 11a) 1.5-m air temperatures at PARMS 2 and ELRE continued to cool at roughly the same rate, but the air temperature at 9 m remained nearly the same value. Thus, the inversion between 1.5 and 9 m increased in magnitude (Fig. 11b).

### d. Skin temperature, upwelling longwave radiation, and net radiation

Net radiation and skin temperature data from the field study showed very consistent trends throughout all 10 cases. Typically, little variation was observed in skin temperature observations between the PARMS during the strong inversions (less than  $2^\circ\text{C}$ ), and the coldest site was predominantly PARMS 4 while the warmest was typically PARMS 3. Upwelling longwave radiation

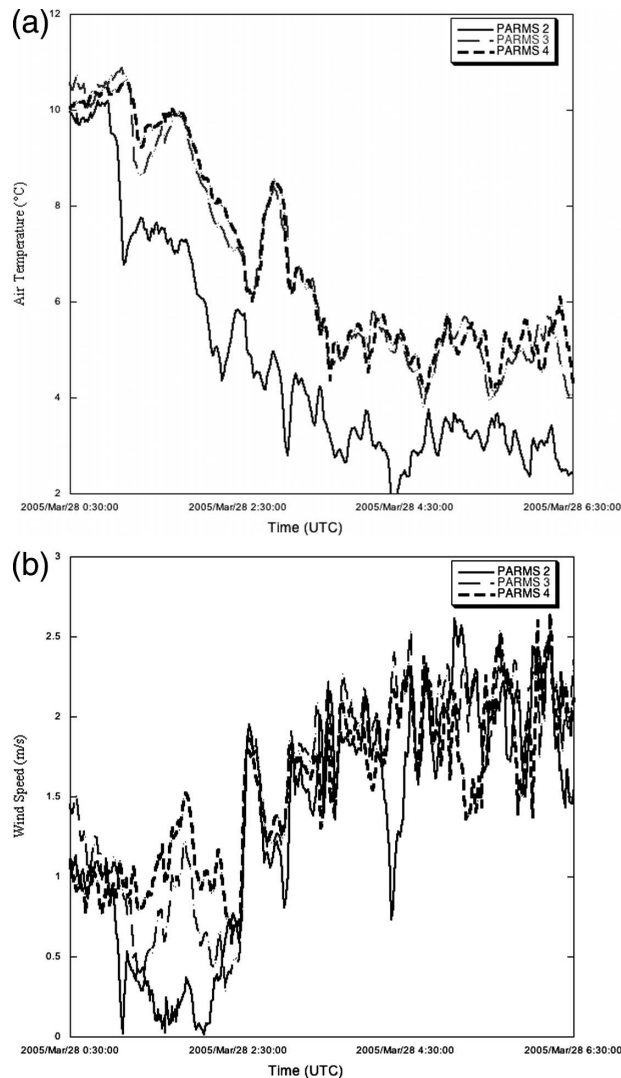


FIG. 10. (a) Air temperature observed by PARMS 2–4 from 0030 to 0630 UTC 28 Mar 2005. (b) Wind speed observed by PARMS 2–4 from 0030 to 0630 UTC 28 Mar 2005.

was estimated from the skin temperature values with the Stefan–Boltzmann equation,

$$E_R = \varepsilon\sigma T^4, \quad (1)$$

where  $\varepsilon$  was equal to 1.0; the emissivity specifically used by the infrared temperature sensor is 1.0 (Fiebrich et al. 2003). As expected from the skin temperature analysis, the differences in upwelling longwave radiation between the PARMS were minimal and typically less than  $10 \text{ W m}^{-2}$  during inversion periods. Further, the greatest longwave emissions were mostly at PARMS 3 while the least typically occurred at PARMS 4. The radiative trends were further confirmed via the total net radiation values observed at each of the PARMS. Again,

during the inversion cases, minimal variability was typically noted and was generally less than  $10 \text{ W m}^{-2}$ . This is not surprising given that in absence of downwelling shortwave radiation and the general lack of turbulent heat fluxes at night, the radiation balance is a function of downwelling and upwelling longwave radiation. As such, because the upwelling longwave showed minimal differences and downwelling longwave radiation is typically homogeneous over limited spatial distances, the temporal variations mirrored the upwelling longwave trends.

The example case from 28 March 2005 demonstrates the typical trends observed throughout the field study. During the inversion period, the skin temperature was slightly warmer at PARMS 3, which resulted in slightly greater upwelling longwave and reduced net radiation values (Figs. 12a,b). Conversely, the skin temperature at PARMS 4 was slightly cooler than the other locations and subsequently the upwelling longwave and increased net radiation values were less (Figs. 12a,b). During the inversion period on 28 March 2005, the radiative variables at PARMS 2 ranged between the values observed at PARMS 3 and 4.

Even though PARMS 2 recorded the coldest temperature values at 1.5 m throughout the field study, the radiation variables did not reveal consistent or similar trends that would identify those specific variables as the reason for the rapid cooling. In fact, the site with the coolest skin temperature values was generally PARMS 4, which typically recorded the greatest temperature values at 1.5 m during inversion periods. It is also important to note the measurement differences associated with the radiation values versus air temperature, humidity, and wind speed. The latter variables represent point measurements of the integrated atmosphere around the sensor with a fetch determined by wind speed and measurement height. The radiation values (net radiation, skin temperature, etc.) utilize sensor technology that observes an integrated footprint on the surface with a diameter spanning a meter or two depending on the sensor's field of view; such sensors are much more likely to be influenced by minor variability in surface conditions.

## 5. Discussion

The analyses from the 5-yr period of historical data and the 3-month field study demonstrated that rapid cooling events led to significant inversions at ELRE. Further, the frequency and strength of the inversions at the surrounding Oklahoma Mesonet sites were rare when compared with ELRE (Table 4). The inversions observed at ELRE were strongly correlated to rapid

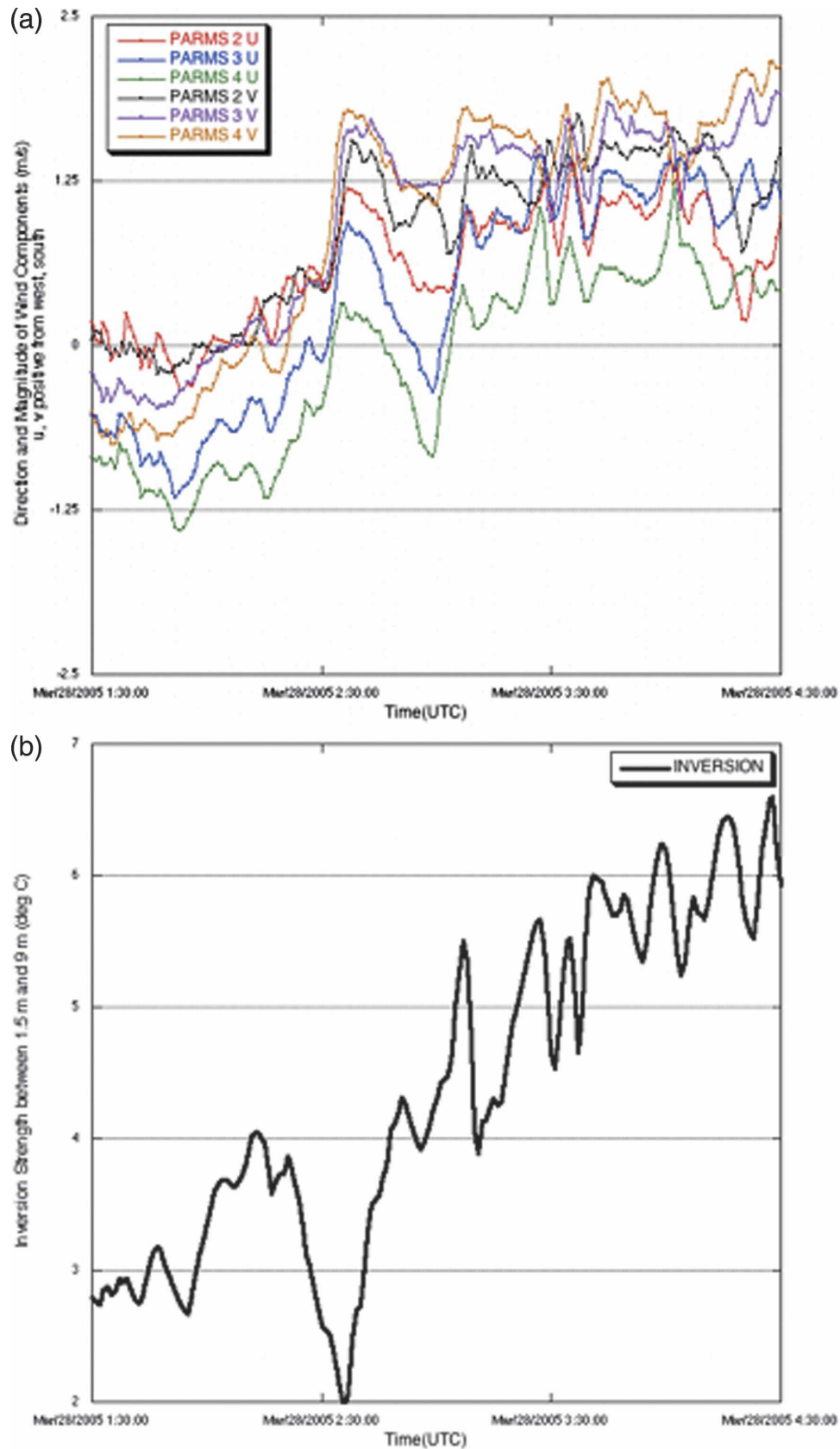


FIG. 11. (a) Wind direction veers to the southwest in the early hours (positive  $u$  and  $v$  components) on 28 Mar 2005. (b) Inversion strength increases as wind direction veers to the southwest on 28 Mar 2005.

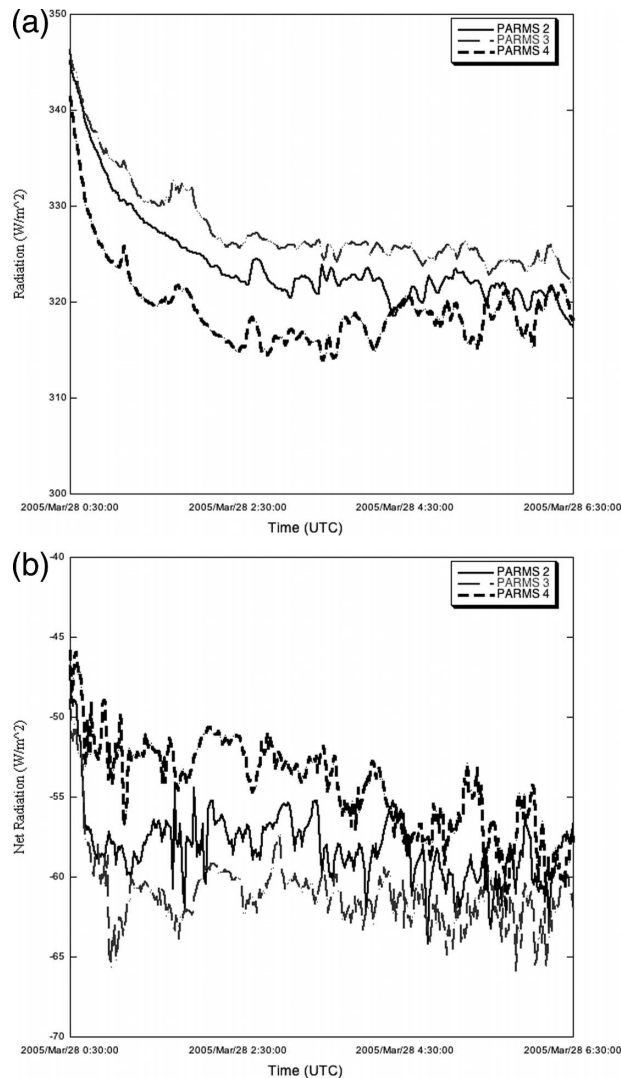


FIG. 12. (a) Estimated upwelling longwave radiation at PARMs 2–4 from 0030 to 0630 UTC 28 Mar 2005. (b) Observed net radiation at PARMs 2–4 from 0030 to 0630 UTC 28 Mar 2005.

cooling near the surface after sunset, and as a result, the atmospheric conditions at ELRE were often very different than surrounding sites during the early nighttime hours (Figs. 6 and 7).

Because the most intense cooling occurred 1) within the first hours after sunset, 2) when wind speed values were nearly calm, and 3) when organized drainage flows were not observed, the most likely cause for the observed conditions was because of in situ cooling. However, in situ cooling has typically been reported in areas that have major obstructions, such as hilly terrain and large trees (Thompson 1986; Gustavsson et al. 1998; Clements et al. 2003). Conversely, ELRE is very well sited by the WMO (WMO 1983) as the slope of the land surrounding ELRE is very minimal (less than 1%)

and the only vegetation surrounding ELRE is natural tallgrass prairie. Yet, rapid in situ cooling seems to occur at ELRE on any night when clear, dry, and calm conditions exist, while not at other surrounding sites.

Even though all three factors are important at ELRE, in situ cooling and the subsequent formation of significant inversions are primarily driven by wind speed. Significant inversions have been observed at ELRE when the dewpoint depression was not large and have occurred when skies were marginally clear. Significant inversions have never formed at ELRE when wind speeds were greater than  $2 \text{ m s}^{-1}$  at 2 m. Thus, 2-m wind speeds at ELRE must be near calm for rapid in situ cooling to occur and strong inversions to form. Further, the analyses revealed that stronger significant inversions (greater than  $6.5^\circ\text{C}$ ) mainly occurred when 2-m wind speeds were less than  $1 \text{ m s}^{-1}$  and borderline significant inversion cases (approximately  $5.5^\circ\text{C}$ ) occurred with wind speed values closer to  $1.5 \text{ m s}^{-1}$ .

The role of wind speed is critical in the formation, maintenance, and erosion of the nocturnal inversion. The results of this study revealed that during the formation of strong inversions at ELRE, significant horizontal and vertical temperature gradients develop at and near the site. Rapid in situ cooling and subsequent formation of the nocturnal inversion occur only when the wind speed values decrease below the critical threshold value of  $2 \text{ m s}^{-1}$  at 2 m. When the winds increase above these thresholds, the mixing causes the temperature gradients to weaken and the low-level nocturnal inversion erodes. The processes responsible for the mixing have not been explicitly quantified in this study and are likely due to a combination of horizontal turbulence, including eddies and shear-induced vertical mixing.

## 6. Concluding remarks

The frequent occurrence of strong inversions and rapid cooling at ELRE is unique when compared with surrounding locations. However, perhaps the most perplexing aspect of the conditions at ELRE is that the rapid cooling and inversion formation occur at a location with minimal terrain and obstructions. As such, the conditions occur at a station that greatly exceeds current WMO siting standards while other locations that are not as well sited do not see such occurrences. The critical results of the study include the following:

- Under most atmospheric conditions, ELRE is very similar to surrounding Oklahoma Mesonet sites. However, under the conditions described in this paper, microscale variability driven by in situ cooling

creates an environment where ELRE is very different from surrounding locations.

- The rapid in situ cooling allows near-surface temperatures measured at 1.5 m to decrease much faster than the observed temperature values at 9 m. As such, significant inversions form because of the large vertical gradient that develops as a result of the rapid near-surface cooling.
- Rapid in situ cooling and the formation of significant inversions have never occurred at ELRE when wind speeds were greater than  $2 \text{ m s}^{-1}$  at 2 m. Additionally, inversions greater than  $6.5^\circ\text{C}$  mainly occurred when 2-m wind speeds were less than  $1 \text{ m s}^{-1}$  and borderline significant inversion cases (approximately  $5.5^\circ\text{C}$ ) occurred with wind speed values closer to  $1.5 \text{ m s}^{-1}$ .
- The field study revealed the presence of strong horizontal temperature differences when wind speeds were very light; half of the cases during the 3-month field study included a  $5^\circ\text{C}$  air temperature difference between sites separated by only a few meters of elevation change and a few hundred meters in distance.
- The results of the field study demonstrated that the skin temperature, upwelling longwave radiation, and net radiation were not well correlated with the trends noted in the rapid cooling at 1.5 m during inversion periods.

The slope of the land surrounding ELRE is minimal. However, the results of this study revealed that the location of the site is situated such that microscale differences in wind speed and air temperature are accentuated under certain environmental conditions. If the site were installed approximately 500 m farther west at the apex of the local terrain (an elevation change of only 10 m), the observed conditions would be dramatically different; the nocturnal 1.5-m temperature values on nights characterized with calm winds, low humidity, and clear skies would be very similar to surrounding mesonet sites.

Long-term consistency of the climate record is a key consideration in the continued monitoring of environmental conditions using the Oklahoma Mesonet. Thus, it is not recommended that ELRE be moved to the apex of the slope or any other location on the property because of temporal inconsistencies that would appear in the climate record at the site. As such, sites like ELRE present a challenge to continuous monitoring of environmental conditions. Further, when analyzing the output of quality assurance tests, it can be difficult to ascertain whether data are valid or erroneous when the scales of representativeness oscillate from very local to regional over relatively short temporal scales.

In the case of ELRE, Oklahoma Mesonet personnel initially responded to the observations of the rapid in situ cooling at ELRE by rotating air temperature sensors between ELRE and other mesonet sites. Once the phenomenon was detected on numerous occasions by multiple sensors, mesonet personnel determined the anomalous observations at ELRE were caused by physical processes and not sensor error. Thus, while the station will not be relocated, because of the prior experiences and the results of this study, information concerning the nocturnal in situ cooling at ELRE is fully documented in the site's metadata. In addition, the knowledge gained is used to validate the removal of automated QA flags directly related to such cooling events.

*Acknowledgments.* Special thanks are given to all members of the Oklahoma Climatological Survey who helped to build and/or deploy the PARMs. Members include David Grimsley, Brad Illston, Peter Hall, Danny Cheresnick, James Southard, James Hocker, Amanda Schroeder, and Scott Stevens. Special thanks also are given to colleagues at the USDA ARS Grazinglands Research Laboratory in El Reno for use of the land surrounding the El Reno Oklahoma Mesonet site, including Herman Mayeux, Jeanne Schneider, and Jean Steiner. Also, the authors greatly appreciate the efforts of Alan Verser, who provided the high-resolution topographic data at ELRE used in this study, and of the anonymous reviewers, who provided significant insight and improved the quality of this paper.

#### REFERENCES

- Ahrens, D. C., 2000: *Meteorology Today: An Introduction to Weather, Climate, and the Environment*. 6th ed. Brooks/Cole, 528 pp.
- Andre, J. C., and L. Mahrt, 1982: The nocturnal surface inversion and influence of clear-air radiational cooling. *J. Atmos. Sci.*, **39**, 864–878.
- Basara, J. B., 2005: Portable automated research micrometeorological stations. Spring 2005 Oklahoma Climate Summary Tech. Memo., Oklahoma Climatological Survey, University of Oklahoma, Norman, OK, 26 pp.
- Brock, F. V., K. C. Crawford, R. L. Elliott, G. W. Cuperus, S. J. Stadler, H. L. Johnson, and M. D. Eilts, 1995: The Oklahoma Mesonet: A technical overview. *J. Atmos. Oceanic Technol.*, **12**, 5–19.
- Clements, C. B., C. D. Whiteman, and J. D. Horel, 2003: Cold-air-pool structure and evolution in a mountain basin: Peter Sinks, Utah. *J. Appl. Meteor.*, **42**, 627–642.
- Feng, J., and Y. Chen, 2001: Numerical simulations of airflow and cloud distributions over the windward side of the island of Hawaii. Part II: Nocturnal flow regime. *Mon. Wea. Rev.*, **129**, 1135–1147.
- Fiebrich, C. A., and K. C. Crawford, 1998: An investigation of

- significant, low-level temperature inversions as measured by the Oklahoma Mesonet. Preprints, *10th Symp. on Meteorological Observations and Instrumentation*, Phoenix, AZ, Amer. Meteor. Soc., 337–342.
- , and —, 2001: The impact of unique meteorological phenomena detected by the Oklahoma Mesonet and ARS Micronet on automated quality control. *Bull. Amer. Meteor. Soc.*, **82**, 2173–2187.
- , J. E. Martinez, J. A. Brotzge, and J. B. Basara, 2003: The Oklahoma Mesonet's skin temperature network. *J. Atmos. Oceanic Technol.*, **20**, 1496–1504.
- , D. L. Grimsley, R. A. McPherson, K. A. Kesler, and G. R. Essenberg, 2006: The value of routine site visits in managing and maintaining quality data from the Oklahoma Mesonet. *J. Atmos. Oceanic Technol.*, **23**, 406–416.
- Geiger, R., R. H. Aron, and P. E. Todhunter, 1995: *The Climate near the Ground*. 5th ed. Vieweg and Sohn Verlagsgesellschaft Publishers, 528 pp.
- Groen, P., 1947: Note on the theory of nocturnal radiational cooling of the earth's surface. *J. Atmos. Sci.*, **4**, 63–66.
- Gudiksen, P. H., J. M. Leone Jr., C. W. King, D. Ruffieux, and W. D. Neff, 1992: Measurements and modeling of the effects of ambient meteorology on nocturnal drainage flows. *J. Appl. Meteor.*, **31**, 1023–1032.
- Gustavsson, T., M. Karlsson, J. Bogren, and S. Lindqvist, 1998: Development of temperature patterns during clear nights. *J. Appl. Meteor.*, **37**, 559–571.
- Hartmann, D. L., 1994: *Global Physical Climatology*. 1st ed. Academic Press, 511 pp.
- Kondo, H., 1995: The thermally induced local wind and surface inversion over the Kanto Plain on calm winter nights. *J. Appl. Meteor.*, **34**, 1439–1448.
- McPherson, R. A., and Coauthors, 2007: Statewide monitoring of the mesoscale environment: A technical update on the Oklahoma Mesonet. *J. Atmos. Oceanic Technol.*, **24**, 301–321.
- Perrotin, H., 1920: Nocturnal cooling of the lower layers of the atmosphere. *Mon. Wea. Rev.*, **48**, 38.
- Shafer, M. A., C. A. Fiebrich, D. S. Arndt, S. E. Fredrickson, and T. W. Hughes, 2000: Quality assurance procedures in the Oklahoma Mesonet. *J. Atmos. Oceanic Technol.*, **17**, 474–494.
- Thompson, B. W., 1986: Small-scale katabatics and cold hollows. *Weather*, **41**, 146–153.
- WMO, 1983: *Guide to Meteorological Instruments and Methods of Observation*. 5th ed. World Meteorological Organization No. 8, World Meteorological Organization, 569 pp.